Isolation and characterization of cellulose nanofibers from aspen wood using derivatizing and non-derivatizing pretreatments

Simon Jonasson · Anne Bünder · Totte Niittylä · Kristiina Oksman

Abstract The link between wood and corresponding cellulose nanofiber (CNF) behavior is complex owing the multiple chemical pretreatments required for successful preparation. In this study we apply a few pretreatments on aspen wood and compare the final CNF behavior in order to rationalize quantitative studies of CNFs derived from aspen wood with variable properties. This is relevant for efforts to improve the properties of woody biomass through tree breeding. Three different types of pretreatments were applied prior to disintegration (microfluidizer) after a mild pulping step; derivatizing TEMPO-oxidation, carboxymethylation and non-derivatizing soaking in deep-eutectic solvents. TEMPO-oxidation was also performed directly on the plain wood powder without pulping. Obtained CNFs (44–55% yield) had hemicellulose content between 8 and 26 wt% and were characterized primarily by fine (height $\approx$ 2 nm) and coarser (2 nm < height < 100 nm) grade CNFs from the derivatizing and non-derivatizing treatments, respectively. Nanopapers from non-derivatized CNFs had higher thermal stability (280 °C) compared to carboxymethylated (260 °C) and TEMPO-oxidized (220 °C). Stiffness of nanopapers made from non-derivatized treatments was higher whilst having less tensile strength and elongation-at-break than those made from derivatized CNFs. The direct TEMPO-oxidized CNFs and nanopapers were furthermore morphologically and mechanically indistinguishable from those that also underwent a pulping step. The results show that utilizing both derivatizing and non-derivatizing pretreatments can facilitate studies of the relationship between wood properties and final CNF behavior. This can be valuable when studying engineered trees for the purpose of decreasing resource consumption when isolation cellulose nanomaterials.

S. Jonasson · K. Oksman (✉)
Division of Materials Science, Luleå University of
Technology, Luleå, Sweden
e-mail: Kristiina.oksman@ltu.se

A. Bünder · T. Niittylä
Umeå Plant Science Centre, Department of Forest
Genetics and Plant Physiology, Swedish University of
Agricultural Sciences, Umeå, Sweden

K. Oksman
Fibre and Particle Engineering, University of Oulu, Oulu,
Finland

K. Oksman
Mechanical and Industrial Engineering, University of
Toronto, Toronto, Canada

Graphic abstract
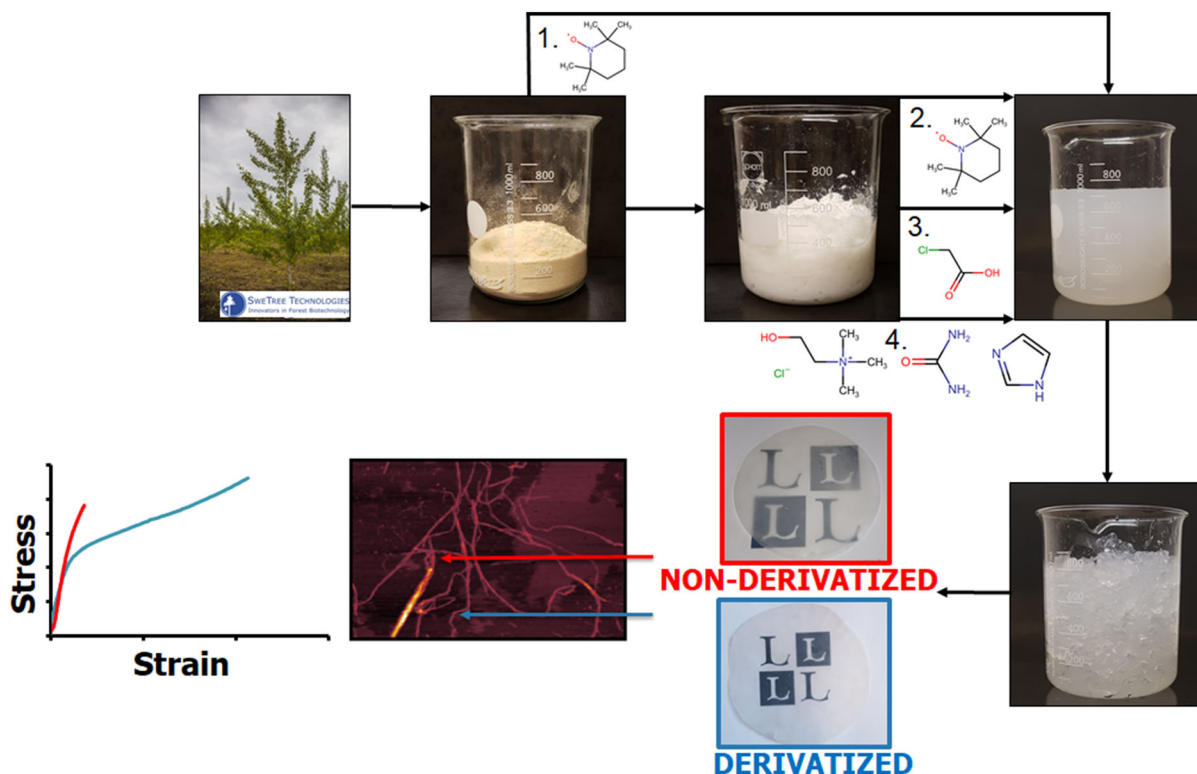
Introduction

Improved processes for isolating cellulose nanofibers
(CNFs) from recalcitrant wood celluloses have
received increased attention recently. The reported
methods include different chemical pretreatments
prior to mechanical disintegration, such as TEMPO-
mediated oxidation (Saito et al. 2007, 2009), enzy-
matic hydrolysis (Henriksson et al. 2007), etherifica-
tion (Wågberg et al. 2008), periodate and chlorite
oxidation (Liimatainen et al. 2012), ionic liquids (Li
et al. 2012), deep eutectic solvents (Li et al. 2017), and
phosphorylation (Noguchi et al. 2017), to name a few.
Aside from significant energy consumption reduction,
enhanced degree of fibrillation is often associated,
where nanofibers resembling the characteristic

individual cellulose micro- or elementary fibrils are
attainable. These resemble the pristine fiber structures
as they are biosynthesized in the plant and show a
range of interesting properties in both suspension and
as solids, whilst also being obtained from renewable
resources. These include biodegradability (Beguin and
Aubert 1994), high mechanical strength (Saito et al.
2013) and stiffness (Iwamoto et al. 2009), optical
transparency (Nogi et al. 2009; Fukuzumi et al. 2009),
and good barrier properties (Syverud and Stenius
2009).

   The pretreatments that are employed for the
isolation of these CNFs are, however, not ideal in
the sense of completely discriminating and separating
the cellulose micro- or elementary fibrils in a quan-
titative manner. The final product can be processed in
either too harsh or too mild conditions relative native
fibril morphologies. The former can be identified as
variable cellulose depolymerisation where corre-
sponding CNFs has been observed to decrease in
length (Shinoda et al. 2012). This has for instance led
to the development of pretreatments that conserve the

degree of polymerization of the nanofibers whilst providing a characteristic high degree of fibrillation (Saito et al. 2010). Other treatments involve cellulose derivatization that irreversibly affects the native cellulose I crystals (Klemm et al. 1998). "Insufficient" treatments in contrast, lead to higher hierarchical fiber retention in the > 100 nm range where elementary fibrils still exist in a highly aggregated state due to the retention of extensive hydrogen bonding (Lepoutre et al. 1976). This has readily has been associated with clogging of the homogenizer during the fibrillation stage (Abdul Khalil et al. 2014).

These broad issues make inquiries regarding the suitability of various woods as feedstocks for CNF production multifaceted, where processing- and property dependencies are difficult to distinguish. The need to relate wood properties to final product quality is of fundamental importance for the development of tailor-made woody feedstock through tree breeding technologies (Zobel and Talbert 1984). For example, decrease in hybrid aspen lignin content has been shown to significantly favor valorization of the biomass with higher yields of biofuels and sugars (Cai et al. 2016). Pulping of gene modified poplars with altered lignin content was shown to decrease the amount of chemicals needed for pulping whilst yielding a pulp with overall better quality (Pilate et al. 2002; Baucher et al. 2003). CNF production from genetically engineered or natural variants of feedstocks is, in contrast to pulping performance or biofuel production, relatively unexplored. In order to increase the understanding of how wood properties influence the isolation of CNFs there is still the need to study the pretreatment procedures in relation to field-grown wood. Through this it may then be easier to conduct large scale wood-to-CNF studies involving a multitude of wood samples with controlled variation in properties.

In this study we tackle these issues through analysis different pretreatments prior to CNF-isolation from one type of clonal field grown hybrid aspen tree. Following a mild pulping step, three different types of pretreatments were tested, namely mild TEMPO-oxidation (pH = 6.8), carboxymethylation and a soak treatment in deep eutectic solvents prior to a mechanical isolation process. In addition, a one-pot process involving direct TEMPO-oxidation (pH = 6.8 and pH = 10) of the wood was also used. This was then compared with the other three treatments in order to

evaluate sample preparation that involves significantly less experimental steps than the more traditional processes. The CNFs from the different treatments were characterized regarding nanofiber morphology, yield, sugar composition, process characteristics and degree of fibrillation. Furthermore, CNF nanopapers (networks) were prepared by filtration and characterized based on their thermal and mechanical properties. The different procedures were then collectively evaluated for their suitability to characterize CNF production from woody feedstocks and were discussed from the context of controlling the link between wood properties and CNF behavior. The aim was to find the most appropriate processing conditions for clonal tree samples that through natural variation or genetic engineering shows differences in wood properties. Through more appropriate processing it is then expected that the relation between tree breeding and isolation of cellulose nanomaterials becomes more pronounced.

Materials and methods

For the CNF-production field grown 5-year-old hybrid aspen *Populus tremula x tremuloides* was supplied by SweTree Technologies AB (Umeå, Sweden) and made into a saw dust. Acetone and methanol with a purity of 99.5% and 99.9% respectively used for dewaxing was purchased by Sigma-Aldrich, Sweden AB. For the treatments, sodium chlorite high purity, with a sodium chlorite content of 77.5–82.5% was purchased from VWR, Sweden. 2,2,6,6-tetramethylpiperidin-1-yl)oxyl 99% (TEMPO), chloroacetic acid $\geq$ 99%, choline chloride (ChCl) $\geq$ 99%, urea $\geq$ 99.5%, imidazole $\geq$ 99%, sodium hydroxide $\geq$ 97%, glacial acetic acid (HAc) 100%, sodium hypochlorite (NaClO, 6–14% active chlorine), sodium bicarbonate (NaHCO$_3$, $\geq$ 99.7%), isopropyl alcohol ($\geq$ 99.7%), sodium bromide ($\geq$ 99%) was purchased from Sigma-Aldrich, Sweden AB. All chemicals were used as received.

Pulping of hybrid aspen

Wood powder ($\sim$ 40 g) was obtained through sawing wood (stem diameter about 3 cm). The powder was dewaxed using acetone/methanol mixture (2:1 wt) in a soxhlet extractor. Mild alkali treatment on extracted

powder was then performed at a liquor:dry powder ratio of 80:1 with a NaOH consistency of 2 wt%. The treatment was performed at 45 °C for 2 h in order to retain large quantities of hemicelluloses to aid in fibrillation (Iwamoto et al. 2008) and to make the cellulose less susceptible to severe oxidation (Tanaka et al. 2016). Conditions were set based on high yield with enough biomass swelling as a function of temperature, time and concentration (data not shown). Delignification of the alkali treated wood was performed according to established protocols (Wise et al. 1947) where three additions of 1 g NaClO$_2$/g$_{wood}$ + 0.2 ml HAc/g$_{wood}$ were added in 1 h intervals. Cooking liqour:dry powder ratio was kept at a 40:1 mass ratio at a temperature of 70 °C. The pulp was filtered both after alkali and bleaching treatment until the conductivity was constant. Quantification of α, β and γ cellulose in extracted wood and pulp was performed by soluble portion in 17.5 wt% NaOH and further precipitation in 3 N H$_2$SO$_4$ according to TAPPI T203 cm-99 "Alpha-, beta- and gamma-cellulose in pulp". Klason lignin was quantified through hydrolysis of the wood powder according to TAPPI T222 om-02 "Acid-insoluble lignin in wood and pulp". The resulting pulp was also analyzed for α-cellulose through soluble portion in 17.5 wt% NaOH.

Pulp pretreatments and CNF isolation

Four types of pretreatments were applied to pulped wood powder, and one pretreatment was applied to the plain wood powder without a distinct pulping step. Carboxymethylation (Wågberg et al. 2008), soaking in deep-eutectic solvents (Sirviö et al. 2015), and TEMPO-oxidation using NaClO$_2$ (Saito et al. 2009) was applied to the pulp whereas TEMPO-oxidation using NaClO$_2$ and TEMPO-oxidation using NaBr (Saito et al. 2006) was applied to the plain wood powder.

Carboxymethylation was performed by solvent exchanging the pulp from water to ethanol using two centrifugation steps. Chloroacetic acid was dissolved in isopropanol and then added to the pulp. After soaking for 30 min the slurry was added to a NaOH/MeOH-solution and treated under reflux at a temperature of 75 °C for 2 h followed by converting the salt from its hydrogen form to its sodium form by addition of NaHCO$_3$ and filtering of the etherified cellulose.

Soaking in DES was performed by suspending slightly dried pulp sheets (∼ 20–30 wt%) in molten mixtures of the components ChCl/Urea or ChCl/Imidazole at a molar ratio of 1:2 and 3:7 respectively. After treatment the slurries were washed thoroughly.

TEMPO-oxidation was performed by first dissolving NaClO$_2$ and TEMPO in the cellulose suspension in the presence of a phosphate buffer (pH = 6.8). The flask was submerged in an oil bath after which NaClO was added and kept at a temperature of 60 °C in a stoppered flask. The suspension was washed after the treatment. Direct TEMPO-oxidation of wood powder was performed in the same manner expect for an increased amount of primary oxidant (5.3 g/g$_{wood}$ instead of 0.7 g/g$_{wood}$) in order to take the presence of lignin into account. Direct TEMPO-oxidation using TEMPO/NaBr/NaClO-system was performed using two individual treatments of 20 mmol/g$_{cellulose}$ each (Saito et al. 2007).

The treated celluloses were diluted to a consistency of 0.2 wt% prior to being disintegrated once in a high shear fluid homogenizer (LM10 Microfluidizer, Microfluidics USA) at 1000 bar. The experimental conditions for respective pretreatment that yielded CNF suspensions and consequently films are shown in Table 1.

Polarized optical microscopy

A Nikon Eclipse LV 100 Pol (Kanagawa, Japan) polarized optical microscope with a 530 nm filter was used to characterize the pulp prior to further treatments and the D-TOCNF suspensions prior to fibrillation. The polarized optical micrographs of the sample were recorded using a charge-coupled device (CCD) camera.

Manufacturing CNF-nanopaper

Nanopapers of the CNF were manufactured by vacuum-filtrating of the prepared suspensions as-obtained from the fibrillation (∼ 200 g) on 90 mm filter paper (Whatman grade 52). When the suspension was structurally intact, after 2–12 h (depending on the CNF grade), they were peeled from the filter paper and cut into 40 mm × 5 mm specimen size using a laser cutter (CMA0604-B-A, Han's Yueming Laser, China). After further air drying for a few hours, they were assembled between two Mylar film-covered

Table 1 Pretreatments applied for wood pulp and powder (D-TOCNF) prior to mechanical disintegration

Denotation	Reagent	Quantity ($m_{reagent}:m_{wood}$)	Conditions	Method
TOCNF	NaClO$_2$	0.7:1	72 h 60 °C	Saito et al. (2009)
D-TOCNF	NaClO$_2$	5.3:1	72 h 60 °C	
CMCNF #1	Chloroacetic acid	0:15:1	2 h 80 °C	Wågberg et al. (2008)
CMCNF #2	Chloroacetic acid	0.60:1	2 h 80 °C	
DESCNF #1	ChCl/Urea	43:1*	2 h 100 °C	Sirviö et al. (2015)
DESCNF #2	Imidazole/ChCl	43:1*	4 h 100 °C	Ren et al. (2016)

*Indicating the cooking liquor:initial wood powder ratio where the liquor consisted of corresponding molten component mixtures

metal plates and pressed with 200 kPa pressure at 120 °C for 15 min using Fontijne Grotnes LPC-300 (Vlaardingen Netherlands). Humidity still present on the nanopapers is thought to act as a plasticizer to even out film inhomogeneities that occur during air-drying. Specimens were considered appropriate if no visible defects were present and retention of optical clarity (if present) was done.

Morphology of CNFs

AFM (Veeco MultiMode scanning probe, Santa Barbara, USA) was used in tapping mode to determine the height of the CNFs. Antimony doped silicon cantilevers (NCHV-A, Bruker) were used with a spring constant of 42 N/m and a nominal tip radius of 8 nm. Height responses (z-axis) were solely used for height-determination of the CNFs in order to avoid misleading dimensions due to tip broadening effects (x–y axes). Samples were prepared by depositing a drop of 0.0015 wt% CNF-suspension on a freshly cleaved mica plate and letting it dry at ambient conditions for a few hours prior to analysis. Obtained micrographs were analyzed in the open-source software Gwyddion (Nečas and Klapetek 2012). The micrographs were presented after image corrections comprising of mean plane subtraction and polynomial background removal.

Nanofibrillated portion

CNF-suspensions ($\sim$ 200 g) were centrifuged at 12,000×g (Beckman Coulter J25i) for 20 min at a consistency of 0.2 wt% (as obtained after fibrillation). The nanofibrillated fraction was decanted and the white sediment was dried for 24 h at 95 °C and then weighted. The nanofraction was calculated according to the equation (Eq. 1) below where m_s is the dry sediment weight and m_t is the total dry weight in the suspension which was obtained by triplicate gravimetric analysis of suspension consistency.

$$Nanofibrillated\ fraction(wt\%) = 100 \times \left(1 - \frac{m_s}{m_t}\right). \tag{1}$$

Mechanical characterization

Mechanical testing of CNF-films was performed using a Shimadzu AG–X universal testing machine (Kyoto, Japan) with a 500 N load cell. Specimens from the CNF-films had the dimensions of 40 mm x 5 mm with thicknesses ranging between 40 and 90 μm. Mechanical testing was performed at a cross-head speed of 10%/min as measured using a video extensometer. 3–5 specimens were measured for each batch of CNF-films. A Q800 DMA analyzer (TA instruments, New Jersey, USA) with a tension clamp configuration was used complimentary to test the stiffness of the CNF films. Three specimens were analyzed for each batch at a strain rate of 1.0%/min at 25 °C.

Turbidity measurements

Turbidity measurements were performed using a Perkin Elmer Lambda2S UV/VIS spectrometer (Überlingen, Germany). The samples used for analysis were the ones obtained from the fibrillation step after dilution (0.164 wt%). Scanning was performed on quartz cuvettes with distilled water as reference in the scanning range between 800 and 200 nm with a data

interval of 0.50 nm. The scan speed was set at 240 nm/min with a smooth setting of 2 nm.

Thermal analysis

Thermal stability of wood, pulp and resulting nanopapers were investigated using thermogravimetric analysis with a TA Instruments TGA-Q500 (New Castle, USA). The analyses were performed at a heating rate of 10 °C/min from room temperature to 700 °C in a nitrogen atmosphere.

Monosugar analysis

Monosugar analysis was performed on wood powder, bleached pulp and the different CNF-films according to an established method (Sweeley et al. 1963). Briefly, the woody biomass and CNF films was grinded and transesterified using 2 M HCl/MeOH followed by silylation using trimethylchlorosilane. The different monosugar derivatives were then quantified using gas chromatography. The original wood powder was used as reference when quantifying the glucose content of the hemicellulosic portion as hydrolysis of cellulose glucose is not necessarily discriminated when analyzing more processed biomass. This was done according to the equation below, where Φ_{sample} is the unknown glucose fraction in the sample, m_{sample} is the wt% of the non-cellulosic sugars and Φ_{wood} is the glucose fraction in the reference wood sample.

$$\Phi_{sample} = \frac{m_{sample}\Phi_{wood}}{(\Phi_{wood} - 1)}. \tag{2}$$

The sugar contents were reported as weight percent of initial dry material. Additionally, the actual glucose content (including that from hydrolysis of the cellulosic solids) was compared between the different nanopapers in order to look at the cellulose digestibility.

Results and discussion

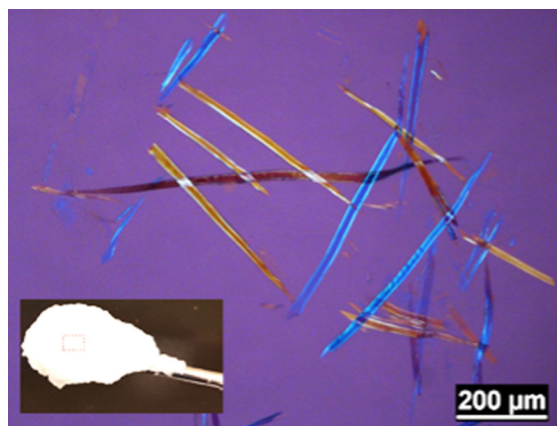### Pulping and chemical composition of hybrid aspen wood

Pulping was intended to be mild in order to keep cell walls intact and retention of additional hemicelluloses

prior to further processing. This was verified by the α-cellulose content of 73% in the pulp. Pulp fibers (640 ± 180 × 20 ± 3 μm) were properly individualized and based on optical micrographs (see Fig. 1) not overly fragmented. This was in accordance with the intent to make the characterization in this study applicable to mildly processed celluloses in order to make the pretreatment step responsible for most of the variation of the resulting CNF and corresponding films. The composition of the wood powder used in the study is shown below in Table 2. Note that the acid soluble lignin portion was not tested which has been reported to comprise around 4 wt% of hybrid aspen (Christiernin et al. 2005).

Pretreatment effect and nanofiber morphology

TEMPO-oxidation of pulp

TEMPO-oxidation (pH = 6.8) with $NaClO_2$ as primary oxidant was deemed as a method with high control of experimental parameters where oxidation is significantly slower and milder than the traditional TEMPO/NaBr/NaClO-system (Saito et al. 2009; Tanaka et al. 2012). Monodisperse CNFs in the lower hierarchical orders were obtained (Fig. 2). The average nanofiber height was measured to 1.7 ± 0.6 nm, reinforcing the more pronounced nanofiber discriminating nature of the treatment where severe polymer degradation, and by correlation, CNF-cleavage (Shinoda et al. 2012) can be limited under certain processing conditions (Saito et al. 2009). From the size


Fig. 1 Optical micrograph and visual appearance of wood pulp as obtained from chlorite bleaching and alkali treatment of wood

Table 2 Chemical composition of the field grown hybrid aspen that was used in the study

Component	Extractives (%)	Klason lignin (%)	α-cellulose* (%)	β-cellulose* (%)	γ-cellulose* (%)
Wood	2.1 (0.3)	15.0 (1.7)	50.0 (0.1)	22.1 (3.2)	28.0 (3.1)
Pulp	–	–	73	–	–

*Based on total polysaccharide content. Standard deviations are shown in parenthesis
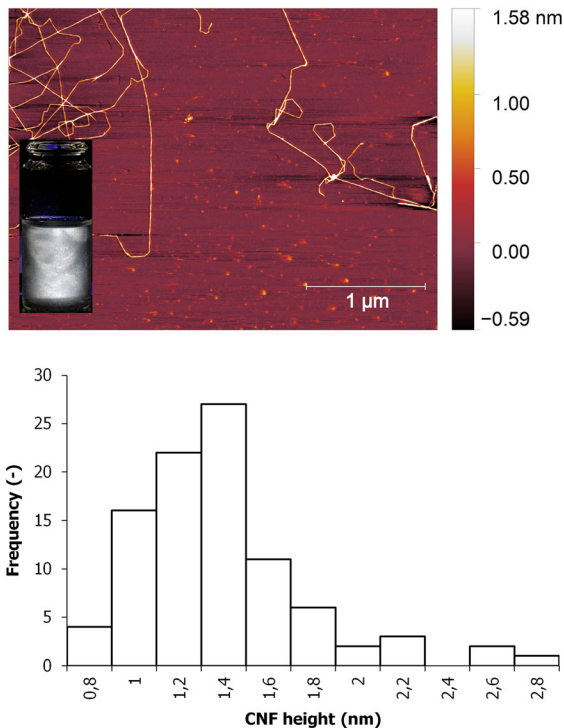
Fig. 2 AFM micrograph and suspension appearance (0.2 wt%) through cross-polarizers (left) of TOCNF with corresponding size distribution (right)

distribution (Fig. 2), minor amounts of small aggregates (2.8 nm) can be seen, likely consisting of few elementary fibrils based on the height difference. Although 3 nm has been attributed to the smallest dimension of wood CNFs, in regard to AFM-analysis there is a clear height difference between 1.7 nm and 3.0 nm, the former value being associated with the characteristic elementary fibril height. Height values of other (< 10 nm) cellulose nanomaterials (cellulose nanocrystals) as observed with transmission electron microscopy (TEM) in relation to AFM has been reported to consistently be a factor of two larger (Jakubek et al. 2018).

Around 95 wt% of the fibrillated suspension was also stable to centrifugation revealing a large nanofractionated portion, i.e. minor amounts of higher hierarchical ordered CNFs (including partly unfibrillated portions). From the aspects of quantifying factors associated with whether cellulose from a certain wood type is appropriate for nanofibrillation this is viewed as positive due to the possibility to relatively easily quantify CNFs of such grade. This is of additional importance given the non-obvious correlation between imaging and degree of fibrillation of CNFs (Lindström 2017).

The yield of CNFs after oxidation was determined to 47.4 ± 0.7%. Yield is expected to be high considering the hemicellulose sparing treatment coupled with an overall minor degradation effect. The yield efficiency of these oxidative treatments has been acknowledged even in the case of the harsher TEMPO/NaBr/NaClO-treatments where yields corresponding to retention of all cellulosic solids have been reported (Isogai and Kato 1998).

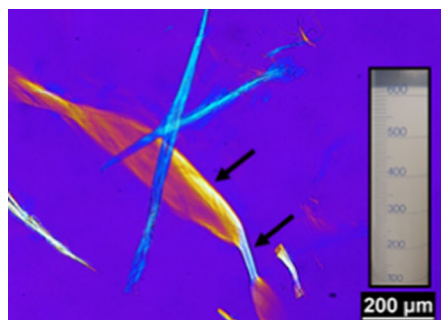### Direct TEMPO-oxidation of wood

The possibility to fibrillate freshly ground wood samples into CNFs of fine grades using one experimental pretreatment was accomplished where the difference compared to the TOCNF-process lies in the need for additional chlorite in order both delignify the wood and oxidize the CNF surfaces to allow for appropriate fibrillation. The exact amount of primary oxidant needed to accomplish similar high degree is expected to be somewhere between 2.5 and 5.2 g/g_{wood} (13–28 mmol/g_{wood}) where the lower interval yielded a product with significant number of visible residues, although seemingly delignified. The time aspect of the treatment was also deemed as an important factor for wood fibrillation as the related TEMPO (pH = 10) treatment, which, despite being more aggressive was found to be non-satisfactory, even after two individual treatments with 20 mmol NaClO per gram of cellulose each. This is seen in

Fig. 3 where lignin and wood structures still were present after the treatment. In contrary, one treatment with 30 mmol/g was enough to directly oxidize hemp bast into disintegrable celluloses with high nanofraction yield (Puangsin et al. 2017). The increased lignin content coupled with native recalcitrance of the wood is likely the cause for incompatibility, or demand for larger amount of NaClO of a direct TEMPO/NaBr/NaClO-treatment. Such treatment has been reported to require a larger amount of NaClO (20–26 mmol/g) when being applied to lignin-containing thermomechanical pulp in order to yield TOCNFs (Okita et al. 2009).
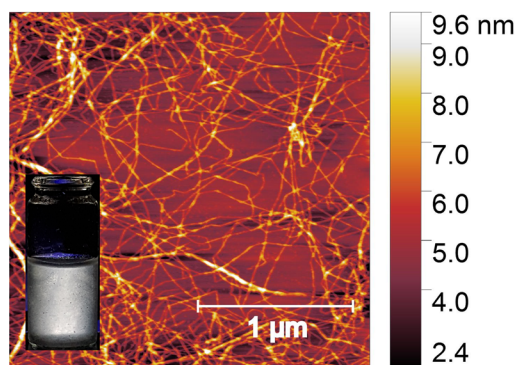
In a similar manner as for the TOCNF-batch rather monodisperse CNFs were obtained according to AFM-micrographs coupled with observed birefringence (see Fig. 4). The height was calculated to 1.6 ± 0.6 nm. Mass yield was estimated to 55 ± 1.0 wt% with a corresponding nanofractionated portion of 85 wt%. Higher yield relative TOCNF was obtained due to increased hemicellulose retention. No significant height variation of the D-TOCNFs was found compared to TOCNFs which indicate that the dimensional aspect of having hemicelluloses still present on the surface (Galland et al. 2015) of the CNFs is as pronounced in TOCNFs as it is in D-TOCNFs. Residual hemicelluloses are likely free in suspension.

Carboxymethylation

More experimental steps are utilized during carboxymethylation than both soaking in DES and TEMPO-oxidation. One difference revolve around the usage of solvent exchange since the reaction is not


Fig. 4 AFM micrograph and suspension appearance (0.2 wt%) through cross-polarizers (left) of D-TOCNF with corresponding size distribution (right)

taking place in an aqueous environment and the seemingly non-discriminating nature of carboxymethylation, the action of which is like the production of non-crystalline carboxymethyl cellulose (Klemm et al. 1998). Carboxymethylation has been optimized for CNF-production without the usage of solvent exchanging and using significantly less reagent (Im et al. 2018), showing on the nuances of

Fig. 3 Optical micrographs and visual appearance of wood particles after direct oxidative treatments (pre-fibrillation) with TEMPO/NaClO/NaClO$_2$ (left) and TEMPO/NaBr/NaClO
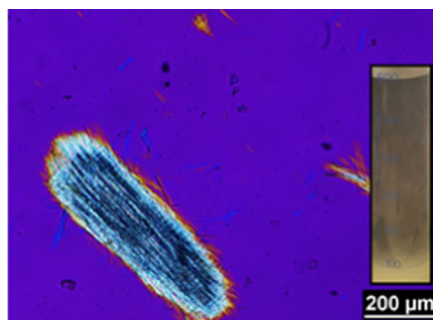
(right). Note the individualization and swelling (arrows) of the wood fibers (left) whereas wood hierarchy from wood powder remaining (right)

the treatment regarding CNF-isolation. With increasing amount of etherification agent (four-fold) the CNFs seemed to bundle together in a fashion indicating loss of rigidity and fibrous integrity, probably an effect of chemical modification within individual cellulose crystallites. This effect has been observed for CMCNFs obtained from beech pulp (Eyholzer et al. 2010). Microscopical observations of this effect are shown in Fig. 5. The height of the CNFs that were observed in both cases was similar at 1.7 ± 0.7 nm and 1.8 ± 0.9 for CMCNF #1 and CMCNF #2 respectively, indicating that the smallest (height) nanofiber structures attainable from wood were obtained. This was also verified by the flow-birefringence Fig. 5 of the suspensions which show homogeneity and individualization of the nanomaterial (De Souza Lima and Borsali 2004).

The yields for both treatments were determined to $50.2 \pm 0.6\%$ and $44.3 \pm 0.8\%$ of initial wood mass for CMCNF #1 and CMCNF #2 respectively. The explanation for the low yields relative the dry content of parent pulp is due to the alkaline nature of the treatment which effectively solubilizes hemicelluloses still present in the pulp. The small variation between the two treatments regarding α-cellulose content furthermore shows that any potential nanofiber derivative was retained during filtration and subsequently part of the final nanofiber film. Including any morphological oddity like those observed in the micrographs.

Deep-eutectic solvent soaking

Soaking in DES had a very low degree of experimental nuisance in the sense that only immersion for a certain period under stirring was required prior to washing and disintegration into CNFs. The treatments used here was rather mild in the sense of obtaining an easy

Fig. 5 AFM micrographs and suspension appearance (0.2 wt%) through cross-polarizers (upper) of CMCNF #1 (left) and CMCNF #2 (right) with corresponding size distributions (lower). Arrows (blue) indicate areas of peculiar nanofiber aggregation where individual nanofibers were resolved within the aggregates
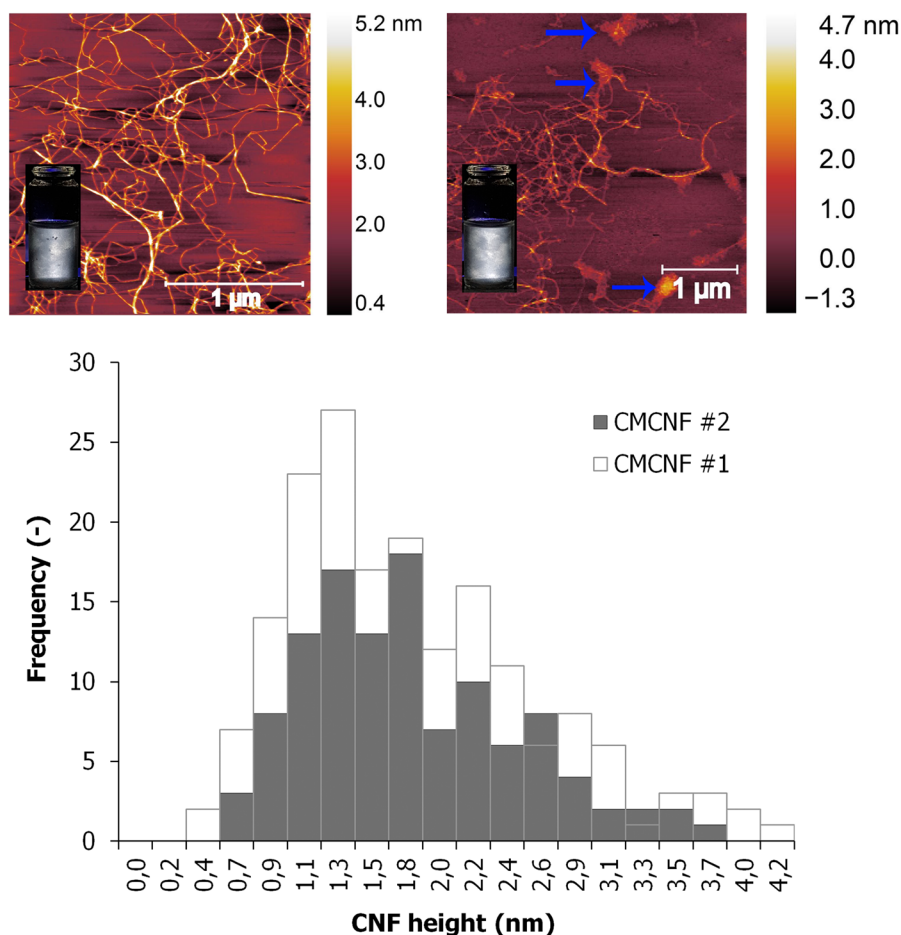
quantifiable product under the current mechanical conditions. Interestingly, cellulose dissolution has been reported using DESCNF #2 treatments, though using cotton linter pulp which was in a less recalcitrant state (Ren et al. 2016). DESCNF #1 treatment for 16 h was reported of having no influence on the pulp fiber morphology (Tenhunen et al. 2018). This may explain the relatively mild effect the treatment (four hours) had on the wood pulp. Further scrutiny using DES-treatments or similar non-derivatizing pretreatments would benefit from multicriteria characterization procedures, for instance according to methods where CNFs of vastly different grades are handled (Desmaisons et al. 2017).

AFM-micrographs are presented in Fig. 6 which shows both a relatively fine fraction of the DESCNFs and that of slightly higher hierarhical order. Finer grades within the suspensions are likely preferentially withdrawn and deposited on the mica sheet and represented to a larger degree in terms of amount of CNFs. The correlation between morphology of CNFs and the content of low hierarchical order CNFs is not nessesarily obvious which further makes conclusions drawn from imaging techniques somewhat convoluted (Lindström 2017). For the fine grade the height was found to be 2.2 ± 1.1 nm and 2.3 ± 1.5 nm for DESCNF #1 and #2 respectively. This shows that geometrically similar nanofibers as those obtained through carboxymethylation and TEMPO-oxidation are attainable (although with a significantly lower yield). Examination of the smallest nanofibers (1.7 nm) further reveal kinking which has been associated with mechanical damage (Saito et al. 2007, pp. 2485–2491) something which has been corroborated further through geometrical analysis of CNFs in relation to sonication procedures (Nyström et al. 2018). Others have additionally attributed the effect to artefacts related to drying rather than inherent properties of cellulose in the traditional sense of disordered and crystalline regions (Funahashi et al. 2017). Explanations in this study may be due to the inhomogenous nature of plant cells where nanofibers within the primary wall and/or S_1-layer are subjected to increased chemical–mechanical stress during the treatment steps compared to those within the deeper S_2 or S_3-layer. In-depth corroborations on this effect likely requires (1) quantification on cellulose content of cell wall layers and (2) appropriate fractionating of the obtained CNFs. Additional explanation may lie in

size dependent features where thinner nanofibers (elementary fibrils) are more seldom observed to bend in a smooth manner because their widths are characterized by one crystallite of high stiffness. This is apparent when looking at the difference in bending behavior between thick and thin nanofibers, both apparent in Figs. 4 and 6. Inherently increased flexibility of larger aggregates consisting of tethered elementary fibrils can consequently be observed.

The yields were determined to $52.2 \pm 0.4\%$ and $43.4 \pm 4.3\%$ for DESCNF #1 and #2 respectively, indicating retention of hemicelluloses in addition to the α-cellulose. Large variation in DESCNF #2 yield can be related to increased efficiency in the dissolution capabilities, which increase the likelyhood of batch-to-batch variations as observed in here. Note that all the material in the final suspension were susceptible to centrifugation, making the nanofibrillated portion difficult to assess. The large difference relative carboxymethylation and TEMPO-oxidation is expected, given the non-derivatising treatment where there are no exogenous charged moeties on the nanofiber surfaces to aid in increased fibrillation and colloidal stability. Additional noteworthy observations include incomplete fibrillation as indicated by Fig. 6a where disintegrated fibers still seems to be physically anchored to the (thicker) CNF from where it originated. This would assist in explaining the high susceptability to centrifugation even amongst the finer fraction.

Monosugar analysis

Sugars from the hemicellulose portion of the wood, pulp and nanopapers are shown in Fig. 7. The main sugars consisted of xylose and glucose followed by 4-O-methylglucuronic acid, galacturonic acid and mannose. Hemicellulose content of around 33 wt% was found in the pulp compared to the 45 wt% of the initial wood specimen. From pulping to final nanopaper production, the hemicellulose content decreased to make up between 8 and 26 wt% of the mass. Hemicellulose content for the different nanopapers was 8.4% (CMCNF), 15.4% (TOCNF), 19.9% (DES) and 26.4% (D-TOCNF). Notable is the high amount of hemicellulose sugars associated with the directly TEMPO-oxidized wood which, in similarity to non-catalyzed chlorite bleaching (Wise et al. 1947) yields holocellulose. Further inspection also reveals the

Fig. 6 AFM micrographs of DESCNF #1 and suspension appearance (0.2 wt%) through cross-polarizers with fine (**a**) and coarse (**b**) portion and DESCNF #2 with fine (**c**) and coarse (**d**) portion. Note the kinking (**b**, black) of the finer nanofibers compared to the smooth bending of the slightly thicker ones (**b**, grey)
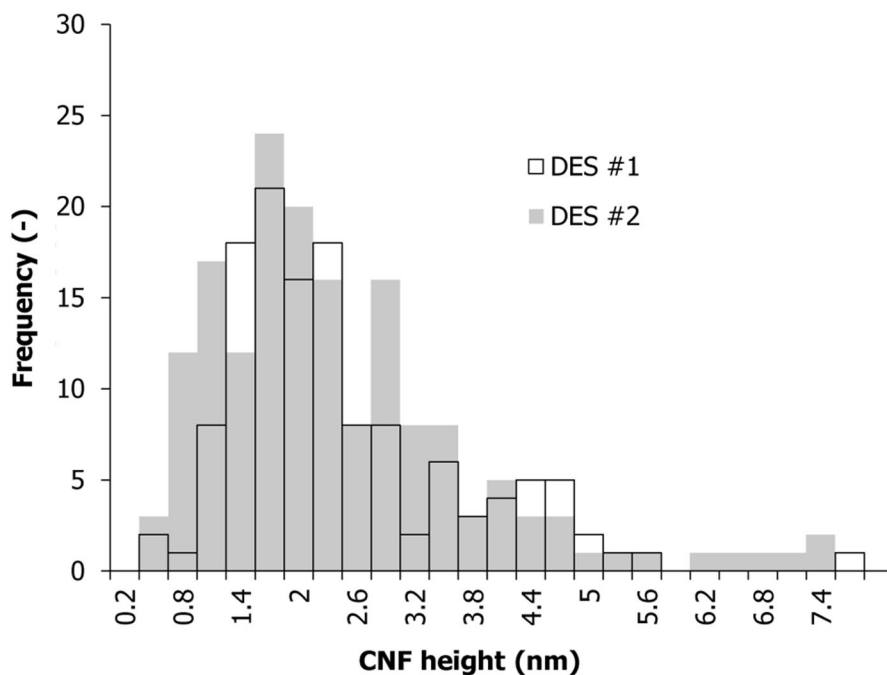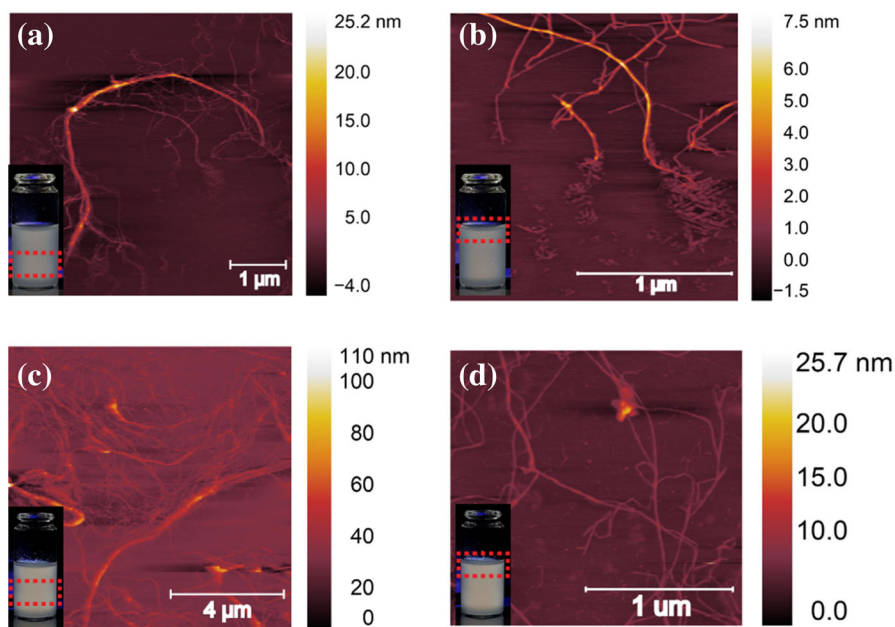
relatively low amount of glucuronic acid, which is a characteristic of oxidation of the C6 primary hydroxyl group. For D-TOCNF it only comprises 0.7 wt% (0.6 mol%) of the final nanopapers compared to the 5.6 wt% (4.9 mol%) of the TOCNF one. D-TOCNF thus has a value closer to the baseline value of the other nanopapers (0.3% $\pm$ 0.1). This indicates that the

TOCNF behavior is not correlated in a trivial way to the conditions used for oxidation. This is further supported (Kuramae et al. 2014) where variations in degree of fibrillation (through turbidity) for different TOCNFs were significantly larger than corresponding variation in degree of oxidation and where the most

Fig. 7 Sugar composition of the hemicellulose portion of initial wood, pulp and the different nanopapers
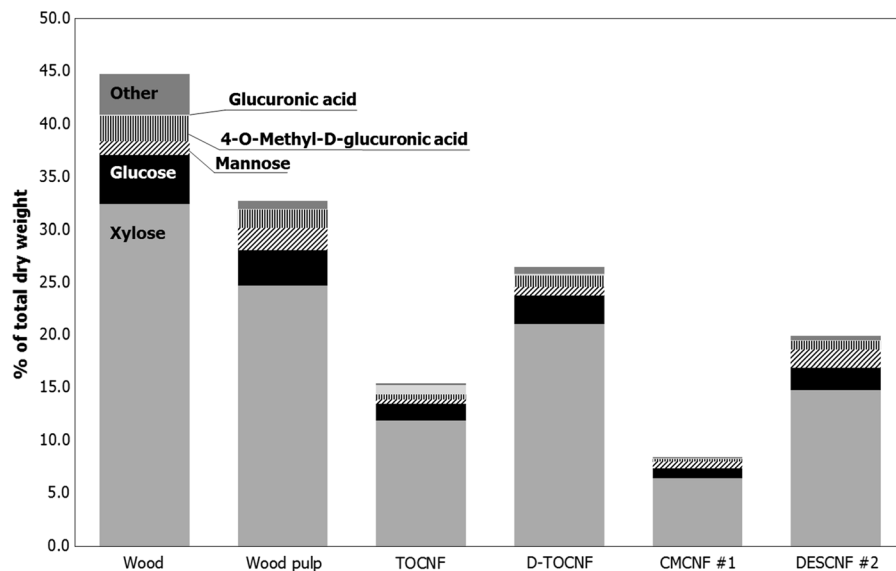
fibrillated sample was not in an obvious way corresponding with the highest degree of oxidation.

The hydrolysis of the samples shows an increased accessibility between pulp and initial wood, likely due increased cellulose fiber exposure during treatment. This can be seen in Fig. 8 where the glucose obtained from hydrolysis is significantly higher than for the other materials. The other samples followed a linear relation ($R^2 = 0.92$) where increased hemicellulose sugar content resulted in less cellulose hydrolysis.

DESCNF #2 seems slightly skewed towards lower glucose, most likely a result of higher hierarchical order, and lower surface area of the nanofibers, inherently being more resistant towards hydrolysis.

Thermal stability of wood and CNFs

Comparing the thermal stability of films made from the CNFs, as presented in Fig. 9 the thermal stability of TOCNF and D-TOCNF is lower than CMCNF

Fig. 8 Relation between glucose obtained from hydrolysis and the hemicellulose content for the different materials. Indication of higher (chemical) biomass recalcitrance with higher hemicellulose is apparent from the trend
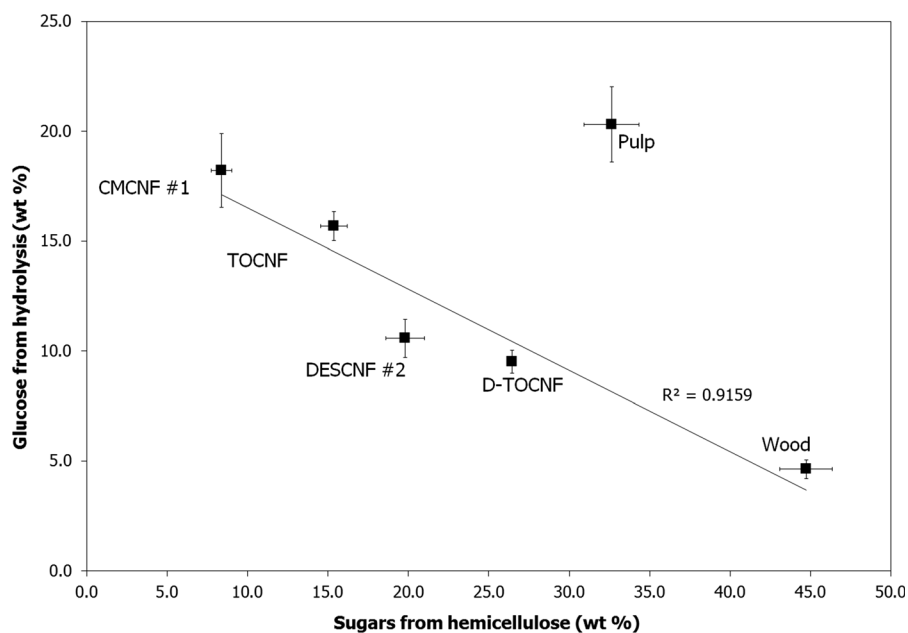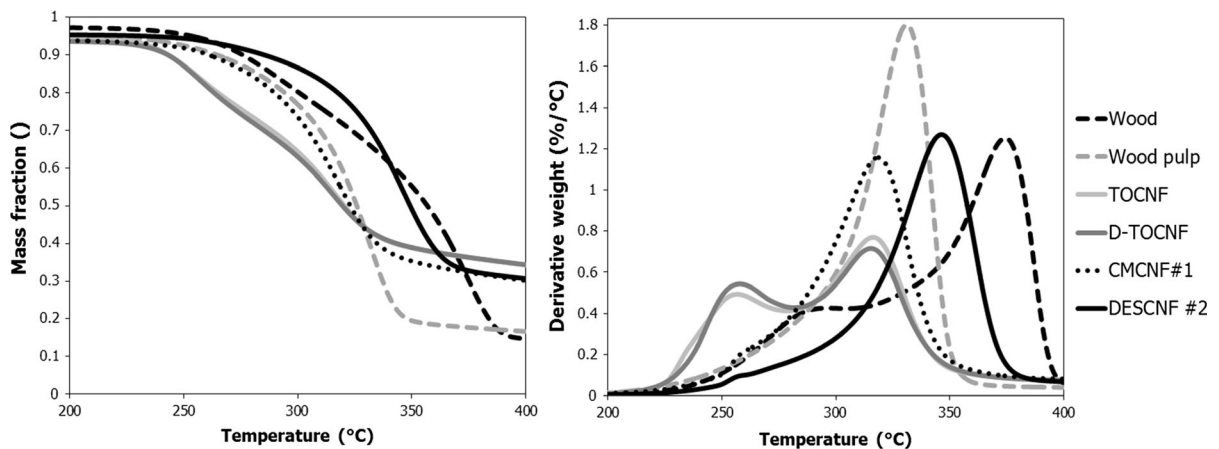
Fig. 9 TGA-graphs of nanopapers, reference wood powder and pulp showing mass fraction (left) and rate of change of mass fraction (right) as a function of increasing temperature

which in turn is lower than DESCNF. The characteristic lower thermal stability of TOCNF can be explained by decarbonation of the oxidized anhydroglucose units (Fukuzumi et al. 2010). CMCNFs have significantly higher thermal stability, which exclusively should be due to the lack of oxidation during treatment since the hierarchical order of the isolated nanofibers are similar as shown earlier Fig. 5 and with the observation of optical clarity and birefringence. The effect of hierarchical structure and absence of chemical derivatization is apparent with the high thermal stability of DESCNFs where the nanofibers can dissipate larger thermal energy before degrading. For the wood and TOCNF/D-TOCNF there seems to be two distinct degradation events. The one for the TOCNFs have been reported to be associated with the degradation of the oxidized and the original cellulose respectively (Fukuzumi et al. 2010). For the original wood it is most likely caused by the difference in degradation of hemicellulose and cellulose where the two components have been reported to be primarily degraded at ~ 220 °C and ~ 315 °C respectively (Yang et al. 2007). The initiation of the thermal degradation of cellulose with an already continuous degradation of hemicellulose then likely causes the overall increased degradation rate. Lignin degradation for the wood can be attributed throughout the whole thermal event and is degrading continuously due to its complex structure. This has been attributed to the plethora of oxygen containing groups of lignin which degrades at different temperatures (Brebu and Vasile 2010). Higher thermal stability of DESCNF

relative starting wood (and pulp) can be explained by different physical forms and chemical composition of tested specimen, which also is reflected in the higher residue content of the films (> 400 °C). Increased cellulose content of DESCNF is also likely to skew the plot into a seemingly singular thermal event despite comprising of around 20 wt% hemicellulose. This can be explained by the resolution under current experimental conditions which is unlikely to resolve these events.

Mechanical properties

The mechanical behavior of the films is presented in Table 3 and was characterized by the similarity of CMCNF and TOCNF where similar tensile strength and stiffness was reached in both cases, even the directly oxidized D-TOCNF nanopaper attained properties like those that had an alkali-bleaching step prior to pretreatment. It should also be emphasized that these similarities are interesting given the large variation in hemicellulose content. This behavior is most pronounced between CMCNF #1 and D-TOCNF films where the difference in low molecular weight polysaccharides is around 18 wt% but corresponding mechanical quantities are indistinguishable ($p > 0.1$). A similar phenomenon has been reported (Galland et al. 2015) where high mechanical properties despite lower cellulose content was attributed to imperfect stress transfer between CNFs in the film, something which was enhanced by the presence of hemicellulose. The stiffness of DESCNFs was significantly higher

Table 3 Mechanical behavior of nanopapers made from CNFs that were extracted from the wood

Sample	Tensile strength (MPa)	Young's modulus (GPa)	Elongation at break (%)
TOCNF	213 ± 24	10.5 ± 1.0	6.1 ± 2.2
D-TOCNF	201 ± 30	10.7 ± 0.9	5.7 ± 1.8
CMCNF #1	219 ± 27	10.1 ± 0.7	5.3 ± 1.5
CMCNF #2	178 ± 38	6.7 ± 0.6	6.3 ± 1.5
DESCNF #1	142 ± 35	12.1 ± 0.3	2.4 ± 0.8
DESCNF #2	119 ± 19	12.9 ± 0.4	2.1 ± 0.5

than that of CMCNF and TOCNF, whereas strength was limited due to low strain-to-break. This can be attributed to inhomogeneous fibrillation where coarser nanofibers (non-uniform fiber size) decreases the number of hydrogen bonds between the fibers and thus resulting in lower elongation and consequently lower strength and toughness.

The results are interesting when comparing fine and coarse grade CNFs, where, in contrary to our results, relatively high elongation-to-break have been reported for coarser grades (Kumar et al. 2014). An explanation for conflicting results may be due to variable homogeneity of the initial CNF suspension where coarse grades do not necessarily imply a homogenous nanofiber size distribution. Possibly originating from the fact that wood with minimal processing preceded mechanical disintegration in this study.

If a process is optimized enough it might liberate a homogenous suspension of a coarser grade CNFs that likely exhibits higher mechanical properties due to the naturally existing filament state of the CNFs which might be(as a bulk material) stronger and stiffer than nanopapers made from individual fine grade CNFs. This is indicated when comparing DESCNF #1 and DESCNF #2 where the former has higher strength and only slightly lower stiffness. Similar increases in strength/elongation-to-break were coupled with larger decrease in stiffness for the fine CNF-films in this study. The behavior is also supported by previously shown AFM micrographs (Fig. 6a, c) that revealed CNFs that were finer than DESCNF #2 yet significantly coarser than TOCNFs.

We did not observe the wood to comply according to ideal scenarios where more intensive processing eventually yields a homogenous CNF suspension. The experimental indication of discourse is the possibility for visible aggregates to exist at the same time as discolored cellulose. Which means that a given cellulose aggregate has recalcitrance strong enough

to degrade rather than fibrillate as a response to mechanical disintegration. DES-treatments makes fibrillation more probable, but whether it has the capacity to result in a homogenous coarse grade CNF at a certain level of aggregation (e.g. 30 nm ± 3 nm) in an analogous way to how TEMPO-oxidation seems to preserve elementary fibrils, remains unexplored. Other DES-based treatments (Li et al. 2017) gave resulting films high strain-to-break which indicates variations based on which specific solvent systems were used, which may expand the potential for DES-treatment as a conservative, coarse grade CNF-isolating method, but also demands systematic studies regarding mechanism, optimization and formulations in order to understand how subsequent crack initiators (Nakagaito and Yano 2004) are removed during fibrillation in relation to "reference" pulp.

The last characteristic of interest is the reduction of tensile strength upon reagent increase (CMCNF #1 compared to CMCNF #2) which indicates that for carboxymethylation there are additional contrasts in terms of processing conditions that can yield films that surpasses optimal conditions in the sense of being too harsh. This type of behavior was not observed with the TOCNFs in the study, which also agrees with early investigators where cellulose derivatives are formed in a different way for oxidative treatments compared to conventional ones (Isogai and Kato 1998). This is an interesting characteristic of TOCNF in the sense of being able to obtain mechanically viable specimens across a wide range of processing conditions. It is on one hand easy to isolate CNFs with a homogenous population but may become difficult to pinpoint exactly how much processing in terms of chemicals and mechanical energy that is required, since the point of maximum fibrillation is readily reached. For instance, with the small amount of disintegration energy needed in the case of strongly oxidized TOCNFs (e.g. 1.5 mmol COO-/g) where frequently

reported disintegration strategies can involve stirring or blending (Isogai et al. 2018) rather than high pressure homogenization that was used in this study.

Turbidity measurements

The turbidity of the CNF-suspensions is presented in Fig. 10 and reflects the varying degree of fibrillation present in the study. The order of the highest transmittance for the CNFs was CMCNF #2 > TOCNF > D-TOCNF > CMCNF #1 > DESCNF #1 > DESCNF #2. The high transmittance for CMCNF #2 in relation to CMCNF #1 is likely slightly inflated by the presence of dissolved polyelectrolyte rather than all the cellulose being in a native fibrous form that can contribute to turbidity in the suspension.

Comparison between TOCNF and D-TOCNF indicates similarities in degree of fibrillation, which is supported by previously shown AFM-micrographs and mechanical tests. Observed flow-birefringence also shows similarities in terms of dispersion, anisotropy of cellulose and its susceptibility to flow alignment (Mtibe et al. 2015). No birefringence can further be seen for DESCNF #1 and #2 with corresponding low transmittance where a spectrum of nanofiber sizes is present. Transmittance is, however, higher for DESCNF #1 compared to #2, where also corresponding tensile strength and elongation-to-break were higher. This indicates a smaller fraction of defects and/or a more homogenous size distribution of CNFs. ChCl/Urea treatments thus seems favorable in
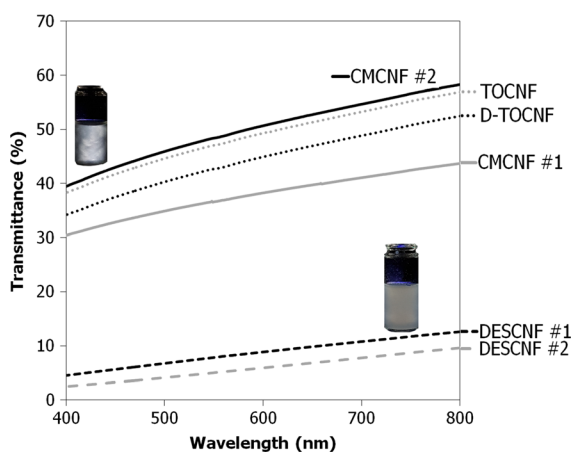
terms of cellulose fibrillation relative to ChCl/imidazole, despite the latter formulation having lower viscosity and having been reported as more efficient for cellulose dissolution (Ren et al. 2016).

Turbidity has been used to estimate widths of nanocelluloses in the < 10 nm range (Shimizu et al. 2016) using developed relationships (Carr and Hermans 1978) which indicate that the fine grade CNFs (D-TOCNFs, TOCNF and CMCNF) varies in average width as a result of variable degree of fibrillation. The overlapping size distributions presented in previous micrographs (Figs. 4, 5, 6) does not necessarily contradict a variable nanofiber width as size distributions most likely is further from being quantitative in relation to turbidity. The presence of a large portion of the finest CNF grades (elementary fibrils) can be confirmed with AFM, but the relative partition of the coarser CNFs is more unreliable and can then be supported with these turbidity measurements. The differences are likely not large enough to influence the mechanical behavior of corresponding nanopapers but might have implications regarding how efficient respective process is when optimizing them individually in regard to a specific wood cellulose and what chemical–mechanical resources are needed.

Outlook on treatment procedures for transgenic specimen

In terms of pretreatment suitability for transgenic and different wood specimen there are different aspects which are conflicted by choice of process as shown in this study through the variety in properties as result of type of treatment and corresponding process characteristics. Fine CNF grades can act as appropriate points of reference for a given sample and process where variations are easily quantifiable at corresponding high degrees of fibrillation. Viscosity differences are for instance quite drastic with a nanofibrillated portion accessible though centrifugation which from this perspective has been acknowledged as a quantitative method (Lindström 2017). Similar fractioning aspect of coarser grade CNFs is more challenging (Larsson Riazanova et al. 2018) and could make characterization of transgenic wood derived CNFs coupled with some additional uncertainty, should the product be primarily comprised of coarse grade CNFs.

The downside, however, with the focus shift from mild or non-existent to more extensive chemical

Fig. 10 Turbidity graphs for 0.164 wt% TOCNFs, D-TOCNF, CMCNFs and DESCNFs with visual appearance through cross-polarizers of derivatized and non-derivatized CNFs apparent

Fig. 11 Illustration of **a** ideal situations where cellulose source and final CNF product are relatable through feedstock properties such as a given phenotype and **b** examples of cumulative errors during each step (red arrows) that makes subsequent steps in the process prone to additional errors
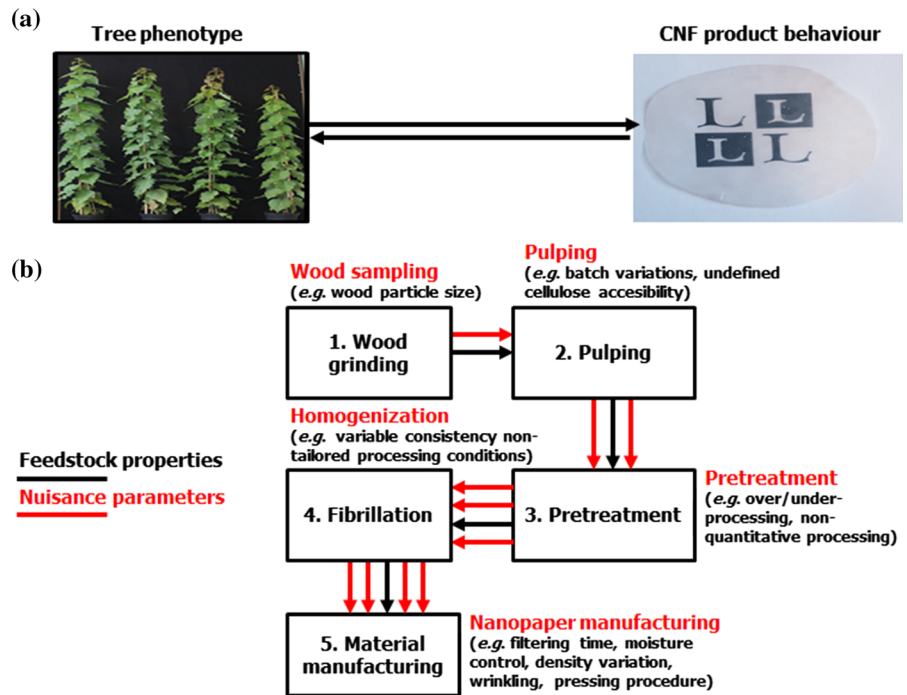
pretreatments is the increased complexity in quantifying factors responsible for influencing the final product. Factors such as bleachability and quantitative chemical requirements may take precedence over the mechanical energy required to obtain a certain grade of CNF. A hypothetical specimen that is easily deconstructed using pure mechanical means might not have an analogous susceptibility to the chemical–mechanical or chemical isolation processes. By ignoring traditional mechanical treatments there is thus the risk of not being able to detect phenotypes related to physical recalcitrance. A good measure is then to consider both mechanical and chemical–mechanical processing, where a selected spectrum of obtained CNFs is obtained with fibrillation efficiency quantified in relation to the respective process and grade of CNFs. In doing so, potential phenotypes related to CNF isolation from wood should be increasingly identifiable, either due to reduced chemical or mechanical recalcitrance.

The D-TOCNFs highlighted in this study touches on the important factor of experimental nuisance. One could for instance argue that individual pulping steps would dictate the susceptibility to further top-down processes in a way that may overshadow sought after contrasts. The CNF behavior derived from two separate commercial sources of wood cellulose would for instance be significantly influenced by the pulping procedure rather than exclusively by inherent wood properties. Bypassing this step would decrease some experimental nuisance in the whole wood-CNF process and allow the shift of the process influence on fewer variables such as time, temperature or amount of $NaClO_2$ (in the case of TEMPO/NaClO/$NaClO_2$). This would result in an overall more controllable process with diminished cumulative error effects. These cumulative errors are inherent to CNF isolation due to the presence of many individual steps and certain non-standardized processing and characterization procedures. These are illustrated below (Fig. 11 b) and does in this context involve everything from whether the wood has been sampled accordingly (e.g. using TAPPI T 257 cm-02 "Sampling and preparing wood for analysis") to making sure manufactured nanopapers have been dried under restriction to avoid wrinkling (Parit et al. 2018).

Under the assumption of experimentally robust processing, the CNF product would then be strongly correlated with initial cellulosic feedstock where recalcitrance would turn into a potentially quantifiable property. It is also possible to tune down the oxidation where it is at a baseline level corresponding to

standard NaClO$_2$-bleaching. This setup would consequently comply with the consideration for *both* mechanical and chemical–mechanical nanofibrillation in order to decipher factors related to lignocellulosic recalcitrance in the context of isolation of CNFs.

Conclusion

CNFs of both fine (height = 2 nm) and coarse grades (2 nm < height < 100 nm) were isolated from field grown hybrid aspen trees using TEMPO-oxidation, carboxymethylation and soaking in DES after a mild pulping step (73% α-cellulose). Fine CNFs with lower content of polyglucuronic acid than TOCNFs were successfully isolated from direct TEMPO-oxidized (pH = 6.8) wood powder; enabling a one-step treatment of wood for experimentally robust CNF isolation with decreased cumulative errors throughout the wood-CNF process.

Nanopapers made from non-derivatizing DESCNFs exhibited higher thermal stability (280 °C) versus 260 °C and 220 °C for CMCNFs and TOCNF/D-TOCNFs, respectively. Stiffness was higher for non-derivatized nanopapers (13 GPa vs. 10 GPa) whereas those from derivatized CNFs had higher tensile strength (200 MPa vs. 140 MPa) and elongation-at-break (6% vs. 2%). CMCNFs were susceptible to over-processing where nanopaper strength and stiffness decreased with large amount of reagent from 220 MPa/10 GPa to 180 MPa/6 GPa which revealed a process-property dependency that was not observed for TOCNFs or DESCNFs. DESCNF nanopapers retained stiffness in relation to higher degree of fibrillation due to preserving the native cellulose hierarchy to a larger extent.

Both types of treatment (derivatizing and non-derivatizing) considerations have important characteristics that can be considered to fully characterize the suitability of wood with different properties for the isolation of CNFs; Fine grade CNFs primarily as a relatively easy quantifiable and characterizable product, and coarse CNFs as a reflection of process efficiency due to a highly variable and more sensitive mechanical response of resulting nanopapers.

References

Abdul Khalil HPS, Davoudpour Y, Islam MN et al (2014) Production and modification of nanofibrillated cellulose using various mechanical processes: a review. Carbohydr Polym 99:649–665. https://doi.org/10.1016/j.carbpol.2013.08.069

Baucher M, Halpin C, Petit-Conil M, Boerjan W (2003) Lignin: genetic engineering and impact on pulping. Crit Rev Biochem Mol Biol 38:305–350. https://doi.org/10.1080/10409230391036757

Beguin P, Aubert JP (1994) The biological degradation of cellulose. FEMS Microbiol Rev 13:25–58. https://doi.org/10.1111/j.1574-6976.1994.tb00033.x

Brebu M, Vasile C (2010) Thermal degradation of lignin—a review. Cellul Chem Technol 44:353

Cai Y, Zhang K, Kim H et al (2016) Enhancing digestibility and ethanol yield of Populus wood via expression of an engineered monolignol 4-O-methyltransferase. Nat Commun. https://doi.org/10.1038/ncomms11989

Carr ME Jr, Hermans J (1978) Size and density of fibrin fibers from turbidity. Macromolecules 11:46–50. https://doi.org/10.1021/ma60061a009

Christiernin M, Ohlsson AB, Berglund T, Henriksson G (2005) Lignin isolated from primary walls of hybrid aspen cell cultures indicates significant differences in lignin structure between primary and secondary cell wall. Plant Physiol Biochem 43:777–785

De Souza Lima MM, Borsali R (2004) Rodlike cellulose microcrystals: structure, properties, and applications. Macromol Rapid Commun 25:771–787. https://doi.org/10.1002/marc.200300268

Desmaisons J, Boutonnet E, Rueff M et al (2017) A new quality index for benchmarking of different cellulose nanofibrils. Carbohydr Polym 174:318–329. https://doi.org/10.1016/j.carbpol.2017.06.032

Eyholzer C, Bordeanu N, Lopez-Suevos F et al (2010) Preparation and characterization of water-redispersible nanofibrillated cellulose in powder form. Cellulose 17:19–30. https://doi.org/10.1007/s10570-009-9372-3

Fukuzumi H, Saito T, Iwata T et al (2009) Transparent and high gas barrier films of cellulose nanofibers prepared by TEMPO-mediated oxidation. Biomacromol 10:162–165. https://doi.org/10.1021/bm801065u

Fukuzumi H, Saito T, Okita Y, Isogai A (2010) Thermal stabilization of TEMPO-oxidized cellulose. Polym Degrad Stab 95:1502–1508. https://doi.org/10.1016/j.polymdegradstab.2010.06.015

Funahashi R, Ono Y, Tanaka R et al (2017) Changes in the degree of polymerization of wood celluloses during dilute acid hydrolysis and TEMPO-mediated oxidation: Formation mechanism of disordered regions along each cellulose microfibril. Int J Biol, Macromol

Galland S, Berthold F, Prakobna K, Berglund LA (2015) Holocellulose nanofibers of high molar mass and small diameter for high-strength nanopaper. Biomacromol 16:2427–2435. https://doi.org/10.1021/acs.biomac.5b00678

Henriksson M, Henriksson G, Berglund LA, Lindström T (2007) An environmentally friendly method for enzyme-assisted preparation of microfibrillated cellulose (MFC) nanofibers. Eur Polym J 43:3434–3441. https://doi.org/10.1016/j.eurpolymj.2007.05.038

Im W, Lee S, Rajabi Abhari A, Youn HL, Lee HL (2018) Optimization of carboxymethylation reaction as a pretreatment for production of cellulose nanofibrils. Cellul 25(7):3873–3883

Isogai A, Hänninen T, Fujisawa S, Saito T (2018) Review: catalytic oxidation of cellulose with nitroxyl radicals under aqueous conditions. Prog Polym Sci 86:122–148

Isogai A, Kato Y (1998) Preparation of polyuronic acid from cellulose by TEMPO-mediated oxidation. Cellulose 5:153–164. https://doi.org/10.1023/A:1009208603673

Iwamoto S, Abe K, Yano H (2008) The effect of hemicelluloses on wood pulp nanofibrillation and nanofiber network characteristics. Biomacromol 9:1022–1026. https://doi.org/10.1021/bm701157n

Iwamoto S, Kai W, Isogai A, Iwata T (2009) Elastic modulus of single cellulose microfibrils from tunicate measured by atomic force microscopy. Biomacromol 10:2571–2576. https://doi.org/10.1021/bm900520n

Jakubek ZJ, Chen M, Couillard M et al (2018) Characterization challenges for a cellulose nanocrystal reference material: dispersion and particle size distributions. J Nanopart Res 20:98. https://doi.org/10.1007/s11051-018-4194-6

Klemm D, Philpp B, Heinze T et al (1998) Comprehensive cellulose chemistry. Volume 1: fundamentals and analytical methods. Wiley, Weinheim

Kumar V, Bollström R, Yang A et al (2014) Comparison of nano- and microfibrillated cellulose films. Cellulose 21:3443–3456. https://doi.org/10.1007/s10570-014-0357-5

Kuramae R, Saito T, Isogai A (2014) TEMPO-oxidized cellulose nanofibrils prepared from various plant holocelluloses. React Funct Polym 85:126–133

Larsson Riazanova AV, Cinar Ciftci G, Rojas R, Øvrebø HH, Wågberg L, Berglund LA (2018) Towards optimised size distribution in commercial microfibrillated cellulose: a fractionation approach. Cellul. https://doi.org/10.1007/s10570-018-2214-4

Lepoutre P, Hui SH, Robertson AA (1976) Some properties of polyelectrolyte-G rafted cellulose. J Macromol Sci Part A: Chem 10:681–693. https://doi.org/10.1080/00222337608061210

Li J, Wei X, Wang Q et al (2012) Homogeneous isolation of nanocellulose from sugarcane bagasse by high pressure homogenization. Carbohydr Polym 90:1609–1613. https://doi.org/10.1016/j.carbpol.2012.07.038

Li P, Sirviö JA, Haapala A, Liimatainen H (2017) Cellulose nanofibrils from nonderivatizing urea-based deep eutectic solvent pretreatments. ACS Appl Mater Interfaces 9:2846–2855. https://doi.org/10.1021/acsami.6b13625

Liimatainen H, Visanko M, Sirviö JA et al (2012) Enhancement of the nanofibrillation of wood cellulose through sequential periodate-chlorite oxidation. Biomacromol 13:1592–1597. https://doi.org/10.1021/bm300319m

Lindström T (2017) Aspects on nanofibrillated cellulose (NFC) processing, rheology and NFC-film properties. Curr Opin Colloid Interface Sci 29:68–75. https://doi.org/10.1016/j.cocis.2017.02.005

Mtibe A, Linganiso LZ, Mathew AP et al (2015) A comparative study on properties of micro and nanopapers produced from cellulose and cellulose nanofibres. Carbohydr Polym 118:1–8

Nakagaito AN, Yano H (2004) The effect of morphological changes from pulp fiber towards nano-scale fibrillated cellulose on the mechanical properties of high-strength plant fiber based composites. Appl Phys A Mater Sci Process 78:547–552. https://doi.org/10.1007/s00339-003-2453-5

Nečas D, Klapetek P (2012) Gwyddion: an open-source software for SPM data analysis. Cent Eur J Phys 10:181–188. https://doi.org/10.2478/s11534-011-0096-2

Nogi M, Iwamoto S, Nakagaito AN, Yano H (2009) Optically transparent nanofiber paper. Adv Mater 21:1595–1598. https://doi.org/10.1002/adma.200803174

Noguchi Y, Homma I, Matsubara Y (2017) Complete nanofibrillation of cellulose prepared by phosphorylation. Cellulose 24:1295–1305. https://doi.org/10.1007/s10570-017-1191-3

Nyström G, Arcari M, Adamcik J et al (2018) Nanocellulose fragmentation mechanisms and inversion of chirality from the single particle to the cholesteric phase. ACS Nano 12:5141–5148. https://doi.org/10.1021/acsnano.8b00512

Okita Y, Saito T, Isogai A (2009) TEMPO-mediated oxidation of softwood thermomechanical pulp. Holzforschung 63:529

Parit M, Aksoy B, Jiang Z (2018) Towards standardization of laboratory preparation procedure for uniform cellulose nanopapers. Cellulose 25:2915–2924. https://doi.org/10.1007/s10570-018-1759-6

Pilate G, Guiney E, Holt K et al (2002) Field and pulping performances of transgenic trees with altered lignification. Nat Biotechnol 20:607–612. https://doi.org/10.1038/nbt0602-607

Puangsin B, Soeta H, Saito T, Isogai A (2017) Characterization of cellulose nanofibrils prepared by direct TEMPO-mediated oxidation of hemp bast. Cellulose 24:3767–3775. https://doi.org/10.1007/s10570-017-1390-y

Ren H, Chen C, Wang Q et al (2016) The properties of choline chloride-based deep eutectic solvents and their performance in the dissolution of cellulose. BioResources 11:5435–5451. https://doi.org/10.15376/biores.11.2.5435-5451

Saito T, Nishiyama Y, Putaux J-L et al (2006) Homogeneous suspensions of individualized microfibrils from TEMPO-catalyzed oxidation of native cellulose. Biomacromol 7:1687–1691. https://doi.org/10.1021/bm060154s

Saito T, Kimura S, Nishiyama Y, Isogai A (2007) Cellulose nanofibers prepared by TEMPO-mediated oxidation of native cellulose. Biomacromol 8:2485–2491. https://doi.org/10.1021/bm0703970

Saito T, Hirota M, Tamura N et al (2009) Individualization of nano-sized plant cellulose fibrils by direct surface carboxylation using TEMPO catalyst under neutral conditions. Biomacromol 10:1992–1996. https://doi.org/10.1021/bm900414t

Saito T, Hirota M, Tamura N, Isogai A (2010) Oxidation of bleached wood pulp by TEMPO/NaClO/NaClO2 system: effect of the oxidation conditions on carboxylate content and degree of polymerization. J Wood Sci 56:227–232. https://doi.org/10.1007/s10086-009-1092-7

Saito T, Kuramae R, Wohlert J et al (2013) An ultrastrong nanofibrillar biomaterial: the strength of single cellulose nanofibrils revealed via sonication-induced fragmentation. Biomacromol 14:248–253. https://doi.org/10.1021/bm301674e

Shimizu M, Saito T, Nishiyama Y et al (2016) Fast and robust nanocellulose width estimation using turbidimetry. Macromol Rapid Commun 37:1581–1586. https://doi.org/10.1002/marc.201600357

Shinoda R, Saito T, Okita Y, Isogai A (2012) Relationship between length and degree of polymerization of TEMPO-oxidized cellulose nanofibrils. Biomacromol 13:842–849. https://doi.org/10.1021/bm2017542

Sirviö JA, Visanko M, Liimatainen H (2015) Deep eutectic solvent system based on choline chloride-urea as a pre-treatment for nanofibrillation of wood cellulose. Green Chem 17:3401–3406. https://doi.org/10.1039/c5gc00398a

Sweeley CC, Bentley R, Makita M, Wells WW (1963) Gas-liquid chromatography of trimethylsilyl derivatives of sugars and related substances. J Am Chem Soc 85:2497–2507. https://doi.org/10.1021/ja00899a032

Syverud K, Stenius P (2009) Strength and barrier properties of MFC films. Cellulose 16:75–85. https://doi.org/10.1007/s10570-008-9244-2

Tanaka R, Saito T, Isogai A (2012) Cellulose nanofibrils prepared from softwood cellulose by TEMPO/NaClO/NaClO2 systems in water at pH 4.8 or 6.8. Int J Biol Macromol 51:228–234

Tanaka R, Saito T, Hänninen T et al (2016) Viscoelastic properties of core-shell-structured, hemicellulose-rich nanofibrillated cellulose in dispersion and wet-film states. Biomacromol 17:2104–2111. https://doi.org/10.1021/acs.biomac.6b00316

Tenhunen T-M, Lewandowska AE, Orelma H et al (2018) Understanding the interactions of cellulose fibres and deep eutectic solvent of choline chloride and urea. Cellulose 25:137–150. https://doi.org/10.1007/s10570-017-1587-0

Wågberg L, Decher G, Norgren M et al (2008) The build-up of polyelectrolyte multilayers of microfibrillated cellulose and cationic polyelectrolytes. Langmuir 24:784–795. https://doi.org/10.1021/la702481v

Wise LE, Murphy M, D'Addieco A (1947) Chlorite holocellulose, its fractionation and bearing on summative wood analysis and studies on the hemicelluloses. Pap Trade J 122:35–43

Yang H, Yan R, Chen H et al (2007) Characteristics of hemicellulose, cellulose and lignin pyrolysis. Fuel 86:1781–1788

Zobel B, Talbert J (1984) Applied forest tree improvement. Wiley, New York